PHYSICAL REVIEW B **83**, 054411 (2011)

Hysteretic behavior and magnetic ordering in CeRuSn

J. A. Mydosh
Kamerlingh Onnes Laboratory, Leiden University, 2300 RA Leiden, The Netherlands and Max Planck Institute for Chemical Physics of Solids, D-01187 Dresden, Germany

A. M. Strydom*
Physics Department, University of Johannesburg, P. O. Box 524, Auckland Park 2006, South Africa and Max Planck Institute for Chemical Physics of Solids, D-01187 Dresden, Germany

M. Baenitz
Max Planck Institute for Chemical Physics of Solids, D-01187 Dresden, Germany

B. Chevalier
CNRS, Université de Bordeaux, ICMCB, F-33608 Pessac Cedex, France

W. Hermes and R. Pöttgen
Institute for Inorganic and Analytical Chemistry, University of Münster, D-48149 Münster, Germany
(Received 7 February 2010; revised manuscript received 11 January 2011; published 9 February 2011)

We report the thermodynamic and transport properties of the newly synthesized Ce-intermetallic compound CeRuSn. This ternary stannide possesses an unconventional structure with two Ce sites at room temperature which exhibit different valencies. Just below room temperature there are large thermal hysteretic effects in the magnetic susceptibility, in the specific heat, as well as in electronic and heat transport properties suggesting the formation of an incommensurate charge density wave modulation whose q vector changes as a function of temperature. Our measurements indicate that one site displays magnetic Ce^{3+} behavior while the other is a valence fluctuator. At 2.7 K antiferromagnetic long-range order occurs within one-half of the Ce sites, e.g., the magnetic entropy of the transition is $\frac{1}{2}R\ln 2$. Below T_N a series of metamagnetic transitions takes place in rather small fields (∼1–2 T), leaving a magnetically fluctuating background. Such behavior is unique among the many Ce–transition-metal compounds.

DOI: 10.1103/PhysRevB.83.054411 PACS number(s): 75.40.Cx, 71.27.+a, 72.15.Qm, 75.20.Hr

I. INTRODUCTION

The class of compounds comprising cerium silicides, germanides, and stannides with transition metals (T), of nominal chemical formula Ce(T)(Si,Ge,Sn) has been an exceptionally profitable research area for exploring novel behaviors.[1] These intermetallic compounds frequently display interesting and unconventional physical properties for which the Ce valency and its variable hybridization with the transition metals are key ingredients. For a review on the ternary equiatomic family to which the title compound is related, the reader is referred to the work of Szytuła and Leciejewicz.[2] The equiatomic compounds also exhibit a variety of correlated electron effects such as intermediate or fluctuating valency, Kondo insulators, quantum phase transitions, and itinerant ferromagnetism coexisting with unconventional superconductivity.

These materials have for many years been the subject of extensive investigation and theoretical attempts to understand or model their behavior.[3–6] One recently synthesized equiatomic compound, CeRuSn, is extraordinary from the structural point of view in that it possesses two distinct Ce sites in its room-temperature structure and below.[7] The focus of the present work is on the unexpected hysteresis behavior of the thermodynamic and transport properties. Such behavior suggests the formation of a first-order charge density wave or even a crystal structure transition below room temperature. This represents a rare addition to the collection of physical properties in cerium compounds that results from the interaction between a more or less localized f-electron magnetic moment, and the degenerate sea of conduction electrons. This highly unusual situation of Ce in a metallic compound warrants full attention to its low-temperature properties both from a structural and electronic or magnetic point of view. We note that the thermodynamic and transport properties, described below, make a case for a CDW scenario. They reflect a strong electron-phonon coupling and alterations in the electronic structure, Fermi surface, and density of states—prerequisities for CDW formation.

Recently, the synthesis and crystal structure of the new stannide CeRuSn[7,8] have been reported. At room temperature, CeRuSn crystallizes with a superstructure of the monoclinic CeCoAl type on doubling of the subcell c axis [isomorphic transition of index 2 with space group $C2/m$, and $a =$ 1156.1(4) pm, $b =$ 475.9(2) pm, $c =$ 1023.3(4) pm, and $\beta =$ 102.89(3)°]. Below room temperature we observe a q-vector modulation along the c axis. Figure 1 shows a projection of the CeRuSn structure onto the ac plane, emphasizing the three-dimensional [RuSn] network. Due to the superstructure formation all three elements now have two distinct, crystallographically inequivalent sites. The corresponding coordination polyhedra for the cerium atoms are presented at the bottom of Fig. 1. For Ce1-Ce1, the nearest-neighbor distances (3.64 Å) and intervening distances of its surrounding Ru atoms are

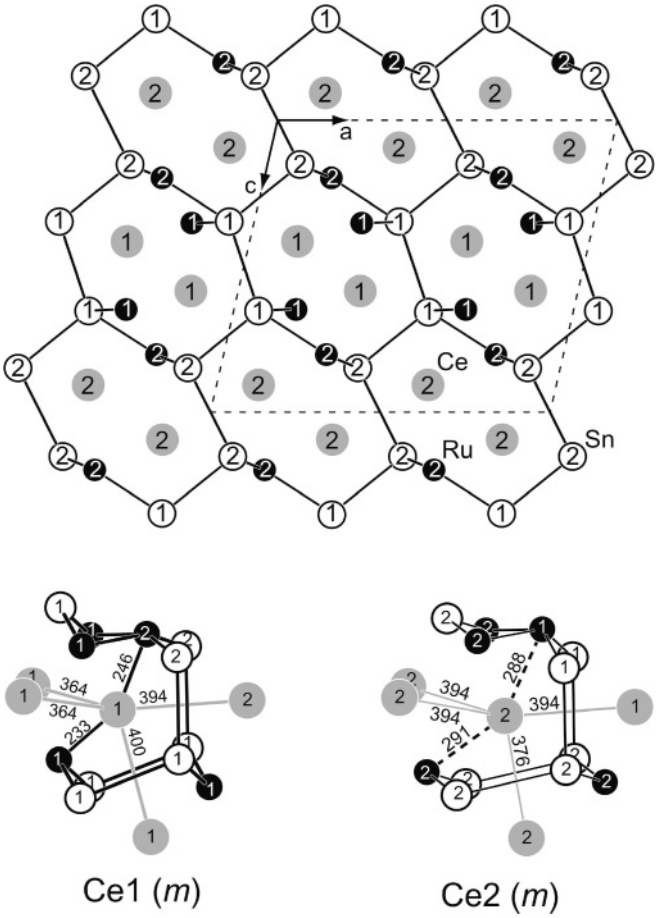

FIG. 1. (Top) Projection of the CeRuSn structure along the monoclinic axis according to Ref. 7. The cerium, ruthenium, and tin atoms are drawn as medium gray, filled, and open circles, respectively. The three-dimensional [RuSn] network is emphasized. The atom numbering for the crystallographically independent sites is given. (Bottom) Coordination of the two cerium sites together with relevant interatomic distances.

significantly smaller than those of Ce2-Ce2 (3.76 Å).[7] This is clearly seen from the polyhedra of the two cerium sites [Fig. 1]. Based on these distinctly different distances and preliminary magnetic susceptibility measurements, it was suggested in Ref. 7 that Ce1 is in an intermediate valent state while Ce2 has the 3+ magnetic valency. This conjecture was supported by electronic structure calculations (DFT) which gave partial density of states values corresponding to the two sites and their distinct valancies.[8] Intermediate valent cerium always leads to extremely short Ce-Ru distances in $Ce_xRu_yX_z$ intermetallics. A further example of such behavior is Ce_2RuZn_4[9,10] and an overview on these peculiar materials is given in Ref. 11.

In order to study both the important high- and low-temperature properties of CeRuSn we have performed magnetic susceptibility, magnetization, and specific heat experiments, along with various transport measurements on the same samples as a function of temperature and magnetic field. Particularly interesting are the large field dependencies of the susceptibility and transport properties for temperatures between 150 and 285 K. The magnetic susceptibility as well as the specific heat, resistivity, and thermopower all show significant thermal hysteresis effects between cooling and heating. We attribute this behavior to the formation of a strongly coupled CDW which begins on cooling at incommensurated wave vector and then possibly locks in to a commensurate one at 150 K. Coexisting CDW and magnetic order are known to exist in various rare-earth- (RE) based tellurides of the form $RETe_2$, $RETe_{2.5}$, and $RETe_3$, including $CeTe_3$.[12] However, these compounds are 2D materials and not strongly correlated. While 3D intermetallics of the $RE_5(Rh,Ir)_4Si_{10}$ type do show coexistence of CDW and antiferromagnetism for most of the rare-earth series, the Ce member of this series does *not* support interpretation in terms of a CDW.[13] A similar two-site Ce-intermetallic compound,[9,10] Ce_2RuZn_4, has been proposed to possess one magnetic Ce^{3+} site and another of intermediate valency that is nonmagnetic. Here one-half of the Ce sites order antiferromagnetic at 2 K but otherwise the bulk properties remain normal without any high-temperature anomalies indicative of CDW or structural modification. Such valence transformations can also be induced by temperature, as recently demonstrated for $CeRh_{0.69}Ir_{0.31}Ge$.[14] Therefore, we consider the putative occurrence of CDW and half-Ce magnetic order in CeRuSn to be highly unusual, if not unique, among the many correlated Ce-intermetallic compounds.

At the lowest temperatures (0.5 K) our experiments indicate long-range antiferromagnetic order ($T_N = 2.7$ K) involving one half of the Ce atoms which is extremely sensitive to rather small magnetic fields of order 1 to 2 T. The field-dependent magnetization exhibits a series of metamagnetic-like transitions which merge into a paramagnetic or fluctuating background.

II. EXPERIMENTAL DESCRIPTION

The synthesis, analysis, and structural determinations of CeRuSn have been given in Ref. 7. See Fig. 1 for the resulting room temperature structure. We used a SQUID technique for susceptibility [$\chi(T)$] and magnetization (M) between 0.5 and 400 K, in magnetic fields between 0.05 and 7 T. The specific heat (C_P) was measured with a commercially available PPMS (Quantum Design, San Diego) for temperatures between 0.35 K and 340 K. Electronic and thermal transport measurements were obtained using the same equipment. Measurement addressing ^{119}Sn nuclear magnetic resonance (NMR) and ^{119}Sn-Mössbauer hyperfine aspects will be the subject of a forthcoming publication.[15]

III. EXPERIMENTAL RESULTS

Figure 2 shows the inverse magnetic susceptibility $\chi^{-1}(T)$, defined as (H/M), as a function of temperature for different magnetic fields. Note that only above 290 K and up to our experimental limit of 400 K does a linear behavior independent of field result. Being a low-field, high-temperature approximation, our $\chi(T)$ data in the upper-temperature phase afford an appropriate analysis of the effective magnetic moment μ_{eff} and the paramagnetic Weiss temperature θ_p. The result of this CW analysis gives $\mu_{\text{eff}} = 1.82\ \mu_B$ and $\theta_p = -10$ K. By comparing this μ_{eff} with that of the free-ion Ce^{3+} value (2.54 μ_B) we find that only 50% of the Ce^{3+}, i.e., $(1/\sqrt{2})2.54\ \mu_B = 1.80\ \mu_B$ are participating as paramagnetic ions in the susceptibility

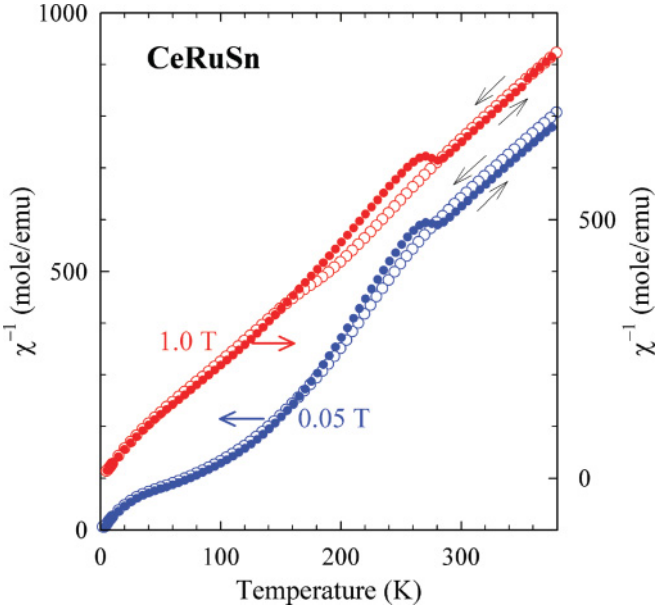

FIG. 2. (Color online) Inverse magnetic susceptibility $\chi^{-1}(T)$ showing the remarkable effect of two different measuring fields, $B = 0.05$ T (blue, left-hand axis) and $B = 1.0$ T (red, right-hand axis) on the susceptibility versus temperature. The thermal hysteretic behavior near the putative CDW formation temperature is emphasized using open symbols for field-cooling (fc) measurements and filled symbols for measurements taken on warming after cooling in zero field (zfc). For clarity, the susceptibility axis of the $B = 1.0$ T data have been displaced by 100 mole/emu.

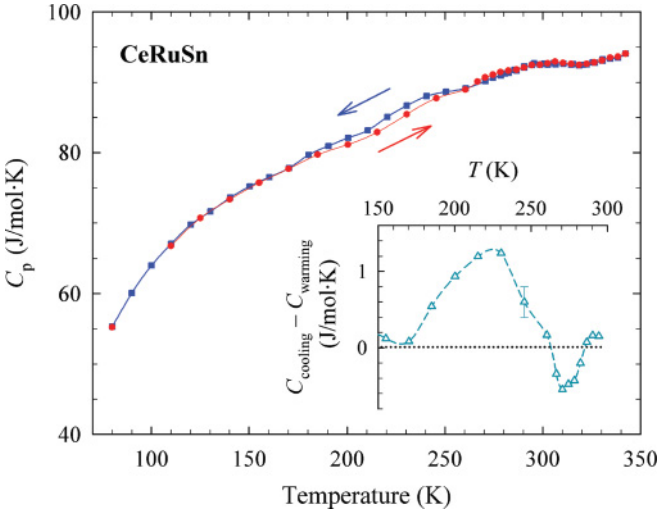

FIG. 3. (Color online) Specific heat of CeRuSn near and below room temperature taken on cooling (blue squares) and subsequent heating (red circles). Several measurement sets have been incorporated into the displayed data to confirm reproducibility. A subtraction of the data under warming conditions from those obtained on cooling is shown in the inset. Lines are guides to the eye.

measurements. So already above room temperature there seems to be a bifurcation of Ce valencies into magnetic and nonmagnetic (fluctuating) components.

Below 290 K the $\chi(T,H)$ behavior is too complicated to enable a meaningful and unambiguous Curie-Weiss analysis. Yet we see that on warming at 285 K there is a clear drop in χ^{-1} (Fig. 2) meaning an increase in χ which we attribute to a Pauli susceptibility $\Delta\chi$ related to an increase in the density of states (DOS) at this temperature. This then suggests a partial gapping or decrease in the low-temperature DOS beginning as one cools below 285 K. The extended hysteresis and strong-field dependencies in the temperature region 150 K to 285 K are most unusual and signify a dramatic sensitivity to local moment magnetism and DOS. It would seem that the crystal structure is undergoing a considerable modification which strongly affects the magnetic behavior, as well as the electronic behavior as will be shown further below.

Hysteresis effects are clearly seen in the specific heat. Figure 3 (main panel) shows results collected on temperature cycling of the sample between 340 K and 80 K despite a large phonon background in this temperature range. Aside from the irreversible behavior of $C_P(T)$ found between $\simeq$170 K and 285 K, one also notes a plateau of temperature-independent specific heat between 295 K and 320 K. To accentuate the difference found between cooling and warming data of $C_P(T)$, we plot in the inset of Fig. 3 the difference $[C_{\text{warming}} - C_{\text{cooling}}]$ as function of temperature. Even though phonons are inevitably making a predominant contribution to C_P at these temperatures, a distinct maximum is resolved at 230 K followed by a minimum at 270 K in the difference curve. These $C_P(T)$ anomalies indicate that entropy and probably latent heat are involved in the hysteretic behavior, which points to the involvement of a first-order transition. Below 150 K, $\chi(T)$ and C_P follow a normal nonhysteretic behavior. However, the strong field dependence evident in $\chi(T)$ that extends to well below 150 K has not yet been examined in C_P.

The electrical resistivity $\rho(T)$ of CeRuSn measured under static thermal conditions is shown in Fig. 4. The resistivity of several samples were measured and a number of consecutive thermal scans (cycling through heating and cooling runs) were conducted in order to verify the reproducible nature of the results in terms of the resistivity values as well as the thermal behavior. In the context of metallic behavior the overall $\rho(T)$ values are comparably large. Whereas the general thermal behavior of $\rho(T)$ is metallic-like with a positive thermal coefficient, the absolute values may not be intrinsic and might be subject to the effects of metallographic defects such as crystallographic grain boundaries and microcracks that develop in an intermetallic compound such as CeRuSn on annealing. The remarkable feature is the thermal hysteretic behavior which is clearly evident in an irreversible loop formed between 160 K and 290 K. The inset in Fig. 4 shows this phenomenon in more clarity in the form of the surplus resistivity in the irreversible region, $\Delta\rho(T) = (\rho_{\text{warming}} - \rho_{\text{cooling}})(T)$.

As a further example of a transport property, the thermopower (a purely electronic effect) of CeRuSn is shown in Fig. 5 with heating and cooling cycles. Note the linear behavior, $\mathbb{S}(T) \sim -T$, as the compound is cooled from 400 K. This relation continues until about 200 K, before the upturn below 190 K. On further cooling, the linear-in-T behavior of $\mathbb{S}(T)$ resumes below 40 K and eventually $\mathbb{S} \to 0$ as $T \to 0$ as is expected from the third law of thermodynamics. Both the negative condition of thermopower throughout the

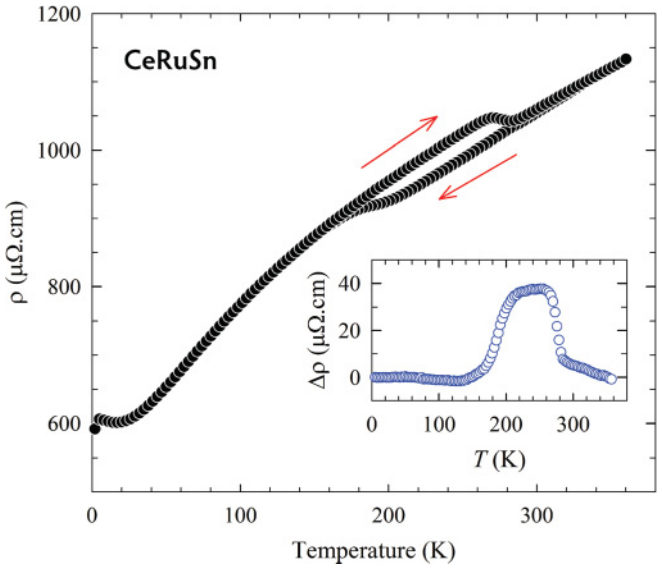

FIG. 4. (Color online) Electrical resistivity $\rho(T)$ of CeRuSn measured on subsequent cooling and warming cycles. Measured under static thermal conditions, the temperature was stabilized at each new point prior to taking a resistivity measurement. The surplus resistivity $\Delta\rho(T) = \left(\rho_{\text{warming}} - \rho_{\text{cooling}}\right)(T)$ formed by the hysteresis loop between 160 K and 290 K is emphasized in the inset.

investigated temperature range, and the $\mathbb{S}(T) \sim -T$ behavior are fundamentally ascribed to a metallic character of the compound. On subsequent warming from 2 K, the three *linear* thermopower intervals in fact turn out to be the *only* temperature regions in which $\mathbb{S}(T)$ is reversible, in the sense that it tracks its behavior on cooling. Between these, a large hysteresis loop is evident. We associate this with a severe disturbance or reconstruction of the Fermi surface or Fermi energy topology, which is a property to which the thermopower is especially sensitive. Similar hysteretic effects were also found in our measurements of the thermal conductivity of CeRuSn (not shown).

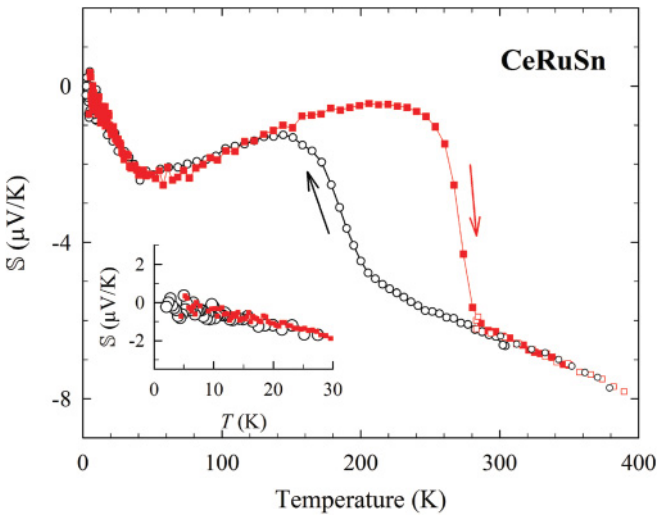

FIG. 5. (Color online) Thermopower $\mathbb{S}(T)$ of CeRuSn measured on cooling (open black circles) and warming cycles (solid red squares). The hystersis loop is bounded by the same hysteretic temperature endpoints as found in susceptibility (Fig. 2) and the specific heat (Fig. 3). (Inset) Approaching low temperatures, $\mathbb{S} \to 0$ linearly in T as $T \to 0$.

At low temperatures, $T < 10$ K, magnetic ordering effects are clearly seen in $\chi(T)$ and M with a sharp peak appearing at about 2.7 K which we attribute to a Néel-type of antiferromagnetic order; see Fig. 6. To obtain a clearer description of the low-T magnetic order we have measured the 0.5 K magnetization as a function of field up to 7 T. From the high-field data in Fig. 7, the Ce moment involved in the magnetism saturates at 0.53 μ_B/Ce. This needs to be compared with the $M = gJ = 2.14$ μ_B/Ce magnetization for all Ce^{3+} ions without crystal electric field splitting or $M = gS = 1$ μ_B/Ce for a CEF ground-state doublet. We note that in the present monoclinic crystal structure the sixfold degenerate $J = \frac{5}{2}$ multiplet of the Ce^{3+} ion may be expected to be lifted into three doublets with energy separations Δ_1 and Δ_2 from the ground state. The fact that the magnetization is very nearly *saturated* at 7 T already suggests that only one doublet is involved in the ground state of Ce^{3+} in either of the two inequivalent sites and that the excited states are situated much higher in energy. Nevertheless, the observed reduced magnetic moment in CeRuSn cannot be explained solely at the hand of a CEF-derived magnetic level splitting. On account of the crystal structure, the partial (1/2) participation of Ce ions per formula unit toward the magnetization is therefore held accountable for the observed deficit in the measured high-field moment in Fig. 7.

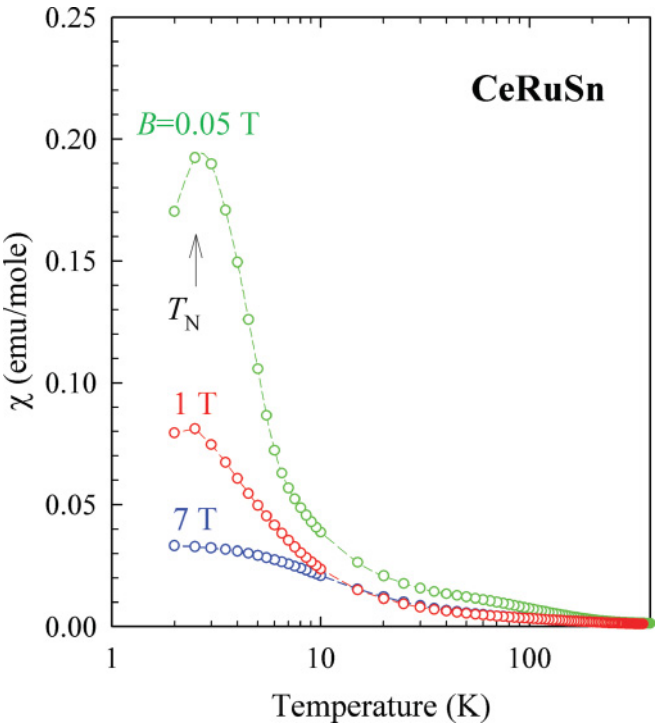

FIG. 6. (Color online) Susceptibility on a semilog plot detailing the antiferromagnetic transition at $T_N = 2.5$ K. The effect of the ordering in $\chi(T)$, as well as a vast suppression of the overall susceptibility is observed as the measuring field is increased.

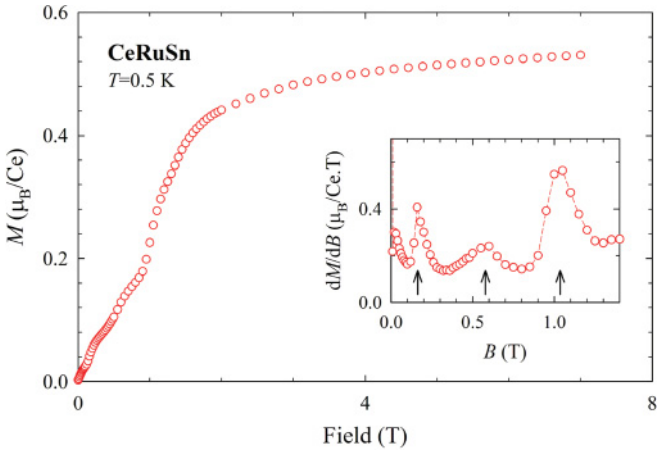

FIG. 7. (Color online) Magnetization as function of field for CeRuSn at $T = 0.5$ K, i.e., well within the antiferromagnetic state. (Inset) Field derivative dM/dB of the magnetization at $T = 0.5$ K emphasizes weak metamagnetic behavior at three field values, marked by arrows.

Closer inspection of the low-field magnetization in Fig. 7 reveals weak metamagnetic-like behavior. This becomes especially evident in the derivative dM/dB versus B plot [see Fig. 7 (inset)], in which three distinct metamagnetic transitions at low fields <2 T (indicated by arrows) are noted. These are typical of a weakly anisotropic antiferromagnet. Data collected at 2 K in fields up to 9 T (not shown) reveal no futher high-field anomalies in the magnetization.

The low-temperature specific heat confirms the magnetic transition with a clear peak that reaches 3.4 J/(mol formula unit)·K at 2.6 K [Fig. 8(a)]. Curiously, the anomaly associated with the ordering transition is rapidly suppressed in height by an applied field of 2 T. Although the magnetic transition anomaly is still evident through the shoulder in $C_P(T)$ in 4 T, the Néel ordering temperature T_N itself does *not* appear to shift significantly with applied field. The entropy of the spin system $S(T)$ is rapidly depleted by applied fields [see Fig. 8(b)]. It is significant that the zero-field entropy well above the ordering

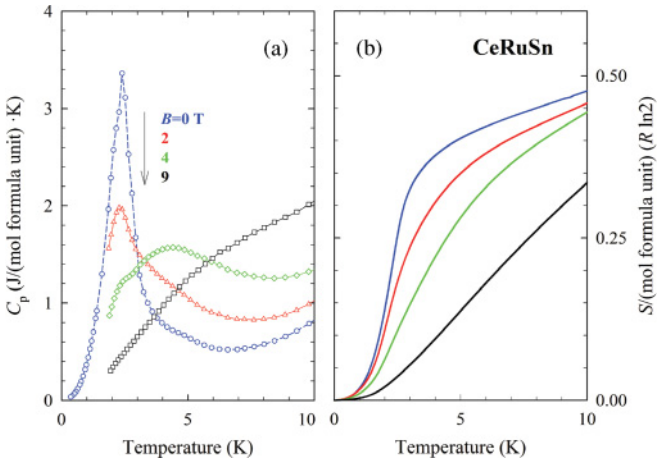

FIG. 8. (Color online) (a) Heat capacity C_p of CeRuSn, per mole of formula unit, at low temperatures in various static applied fields. (b) Calculated entropy, in units of $R \ln 2$ per mole of formula unit, in fields corresponding to those shown in (a).

temperature reaches no more than about $\frac{1}{2}R \ln 2$. We ascribe this to a $\frac{1}{2}$-fractional contribution of the cerium atoms per formula unit contributing to the magnetic entropy, a finding which also asserts the fractional participation of cerium ions in the high-temperature paramagnetism of CeRuSn.

IV. DISCUSSION AND CONCLUSION

Based on the present experimental situation we propose the following conclusions: CeRuSn exhibits a novel crystal structure, unique among the equiatomic ternaries, already at and above room temperature. According to low-temperature x-ray diffraction (XRD) the structure is modified along the *c* axis below room temperature. Here two Ce sites are indicated with different valencies and magnetic states, i.e., local moment and valence fluctuator. A superstructure modulation occurs just below room temperature as detected by large hysteretic changes in all the bulk (thermodynamic and transport) properties. We attribute this behavior to the slow formation of a charge density wave in this compound with cooling and rapid demise on heating to around 290 K. The CDW is probably incommensurate and strongly coupled both to the lattice and to the electronic and magnetic properties. A clear antiferromagnetic transition takes place at 2.7 K that involves only ~50 at % of the cerium atoms and with metamagnetic-like modifications occurring in low fields.

According to the above we have provided additional experimental support for the conjectures put forth in Refs. 7 and 8 that, due to the two-site Ce structure, there exist $\frac{1}{2}Ce^{3+}$ (magnetic) and $\frac{1}{2}Ce^{(3+\delta)+}$ (intermediate or fluctuating valence) states. In an intermetallic compound two distinct and coexisting Ce sites are not intuitive, for both sites are embedded in a sea of conduction electrons which should hybridize out their differences. Nevertheless, as shown in Fig. 1 there are significant changes in the local environment surrounding the two Ce sites and according to Ref. 8 their partial densities of states are severely modified, both indicative of the differing valencies.

In order to further investigate this intriguing puzzle we are continuing with experiments such as Hall effect and thermal expansion, NMR and Mössbauer effect on ^{119}Sn as a local probe.[15] X-ray absorption spectroscopy and x-ray photoelectron spectroscopy are needed to establish the Ce valencies and synchrotron XRD to detect the putative CDW and denote its propagation vector.[16] Most important is that one has to verify a CDW formation via the observation of temperature-dependent incommensurate superstructure lines in single-crystal XRD.[16] In addition, powder neutron diffraction at and below 1 K will be carried out to determine the antiferromagnetic structure. We are also investigating the growth of single crystal material as required for some of the above experiments.

ACKNOWLEDGMENTS

We have benefited from useful discussions with R. Feyerherm, and K. Prokes. W. Hermes is indebted to FCI for a PhD stipend. A. Strydom acknowledges funding support from the SA-NRF (2072956), the German DFG (OE511/1-1), and from the Science Faculty at UJ.

*amstrydom@uj.ac.za

[1]G. R. Stewart, Rev. Mod. Phys. **73**, 792 (2001).

[2]A. Szytuła and J. Leciejewicz, in *Handbook of Crystal Structures and Magnetic Properties of Rare Earth Intermetallics* (CRC Press, Boca Raton, FL, 1994), p. 83.

[3]For example, see: *Proceedings of the International Conference on Strongly Correlated Electron Systems*, Physica B **404** (2009), and SCES (2010), to be published in J. Phys.: Conf. Series.

[4]A. A. Al Alam, S. F. Matar, N. Ouaini, and M. Nakhl, Eur. Phys. J. B **65**, 491 (2008).

[5]H. Higaki, I. Ishi, D. Hirata, M.-S. Kim, T. Takabatake, and T. Suzuki, J. Phys. Soc. Jpn. **75**, 024709 (2006).

[6]A. Ślebarski, K. Szot, M. Gamża, H. J. Penkalla, and U. Breuer, Phys. Rev. B **72**, 085443 (2005).

[7]J. F. Riecken, W. Hermes, B. Chevalier, R.-D. Hoffmann, F. M. Schappacher, and R. Pöttgen, Z. Anorg. Allg. Chem. **633**, 1094 (2007).

[8]S. F. Matar, J. F. Riecken, B. Chevalier, R. Pöttgen, A. F. Al Alam, and V. Eyert, Phys. Rev. B **76**, 174434 (2007).

[9]V. Eyert, E.-W. Scheidt, W. Scherer, W. Hermes, and R. Pöttgen, Phys. Rev. B **78**, 214420 (2008).

[10]R. Mishra, W. Hermes, U. Ch. Rodewald, R.-D. Hoffmann, and R. Pöttgen, Z. Anorg. Allg. Chem. **634**, 470 (2008).

[11]W. Hermes, S. F. Matar, and R. Pöttgen, Z. Naturforsch. B **64**, 901 (2009).

[12]See, for example, D. A. Zocco, J. J. Hamlin, T. A. Sayles, M. B. Maple, J.-H. Chu, and I. R. Fisher, Phys. Rev. B **79**, 134428 (2009).

[13]S. Ramakrishnan and J. A. Mydosh, J. Magn. Magn. Mater. **310**, 207 (2007).

[14]E. Gaudin, B. Chevalier, B. Heying, U. Ch. Rodewald, and R. Pöttgen, Chem. Mater. **17**, 2693 (2005).

[15]M. Baenitz, J. A. Mydosh, A. M. Strydom, B. Chevalier, W. Hermes, F. M. Schappacher, J. F. Riecken, and R. Pöttgen (to be published).

[16]R. Feyerherm and S. Valencia (private communication and to be published).